Hindawi
Journal of Chemistry
Volume 2023, Article ID 2581653, 10 pages
https://doi.org/10.1155/2023/2581653

Research Article

Binding Investigation of Some Important Metal Ions Copper (I), Nickel (II), and Aluminium (III) with Bovine Serum Albumin Using Valid Spectroscopic Techniques

Hassan A. Alhazmi,[1,2,3] **Md Shamsher Alam**,[1] **Mohammed Albratty**,[1] **Asim Najmi**,[1] **Ahmed A. Abdulhaq**,[4] **Rym Hassani**,[5] **Waquar Ahsan**,[1] **and Abdulrahman N. Qramish**[6]

[1]*Department of Pharmaceutical Chemistry and Pharmacognosy, College of Pharmacy, Jazan University, P. Box No. 114, Jazan, Saudi Arabia*
[2]*Substance Abuse and Toxicology Research Centre, Jazan University, P. Box No. 114, Jazan, Saudi Arabia*
[3]*Medical Research Center, Jazan University, Jazan, Saudi Arabia*
[4]*Medical Laboratory Technology Department, College of Applied Medical Science, Jazan University, Jazan, Saudi Arabia*
[5]*Nursing Department, University College of Sabya, Jazan University, Saudi Arabia*
[6]*College of Pharmacy, Jazan University, P. Box No. 114, Jazan, Saudi Arabia*

Correspondence should be addressed to Md Shamsher Alam; mosalam@jazanu.edu.sa

Received 18 October 2022; Revised 4 January 2023; Accepted 19 January 2023; Published 15 February 2023

Academic Editor: Davut Avci

Studies based on the interaction of metals with proteins resulted in the development of promising metal-based compounds with encouraging medicinal potential. This study was aimed to utilize FT-IR and UV-Vis spectroscopic techniques to analyze the interactions of biologically significant metal ions, such as Al^{3+}, Ni^{+2}, and Cu^{+}, with bovine serum albumin (BSA). Different concentrations of metal ions were interacted with BSA, and the complexes were analyzed using the two techniques. The change in the BSA secondary structure components such as β-sheet, β-antiparallel, α-helix, β-turn, and random coil were analyzed using second derivative resolution enhancement. The FT-IR spectroscopy suggested a marked decrease in the C=O stretching (corresponding to amide I) and C=N stretching (corresponding to amide II) intensities. Interestingly, upon complexation, a marked reduction (22.58–29.03%) in the α-helical component was observed with a considerable increase in the random coil component. The intensity of the absorption peak of BSA obtained using UV was observed to increase consecutively as the concentration of Cu^{+}, Al^{3+}, and Ni^{2+} ions increased. The binding constants for the BSA-Cu^{+}, BSA-Ni^{+2}, and BSA-Al^{+3} complexes were calculated to be $3.46 \times 10^4\ M^{-1}$, $1.28 \times 10^4\ M^{-1}$, and $2.08 \times 10^4\ M^{-1}$, respectively. It was concluded that the binding interaction decreased in the order $Cu^{+} > Al^{3+} > Ni^{2+}$. These findings were similar to our previous findings using affinity capillary electrophoresis (ACE). Therefore, it can be inferred that the FT-IR and UV techniques might be utilised effectively to assess the metal-protein interaction and can have wide application in routine analysis. These techniques have several advantages in being simple, easy-to-perform, rapid, and affordable over other high-end techniques.

1. Introduction

Albumin, the most prevalent plasma protein, accounts for almost 60% of the total plasma protein content in vertebrates. Owing to its widespread accessibility and similarity (76%) with human serum albumin (HSA), bovine serum albumin (BSA) is widely used to investigate the binding of biologically active molecules to the albumin protein [1]. The BSA protein molecule is made up of a single chain consisting of 583 amino acids bonded together with 17 cysteine residues and has a molecular weight of 66400 Da. The structurally different domains I, II, and III, consisting of chains of various amino acids, are separated

Figure 1: Three-dimensional structure of simple BSA protein (downloaded from protein data bank; ID: 4F5S (https://www.rcsb.org/).

into nine loops, which are connected by disulfide bonds (Figure 1). Two subdomains (A and B) are also included in each domain. The peptide chain is made up of turns that are extended between the subdomains, while secondary structure is primarily composed of α-helices and β-sheets [2].

Since metal ions play a significant role in many biological processes, researchers have long found studying protein-metal ion interactions to be fascinating. Metalloproteins along with other proteins, have the affinity to interact through some of the metal ions, and their selectivity is crucial as some of these interactions have physiological and pathological implications [3, 4]. Biomolecules such as proteins have a strong affinity for bioinorganic complexes, and this potential is widely utilised for designing active compounds that can combat bacterial, fungal, and viral diseases and even can treat a variety of tumors [5]. For instance, the effectiveness of platinum-based anticancer agents such as carboplatin and cisplatin in the treatment of various cancers has already been established.

The ability of analytical techniques for the measurement of metal-protein interactions rely on a number of variables, including sensitivity, accuracy, precision, timeliness, scale of analysis, ability to operate under physiological conditions, sample complexity, as well as method complexity while selecting the best analytical approach, all these considerations should be made. Generally, the most difficult aspect of each approach is the intricacy of the sample and its preparation. Nuclear magnetic resonance (NMR), surface plasmon resonance (SPR), thermal shift assay, affinity capillary electrophoresis (ACE), X-ray crystallography, atomic force microscopy (AFM), circular dichroism (CD), and other analytical methods have all been used previously to effectively measure these interactions [6–8]. Recently, Fourier transform-infrared (FT-IR) spectroscopy has emerged as a useful tool for measuring these interactions, and it has produced promising results that are comparable to those of other top-tier analytical methods [2].

Previously, our research team has been involved in the investigation of binding of various monovalent, divalent, and trivalent metal ions, drugs, and various other molecules with different proteins using a number of techniques, and some promising findings were reported [2, 9–12]. We have recently been researching the application of spectroscopic techniques such as FT-IR and UV-Vis to detect metal-protein binding interactions and compare the results with other sophisticated techniques. We tested the effects of various biologically significant metal ions on the BSA protein using FT-IR and UV-Vis spectroscopy in order to identify the binding sites and measure the strength of interactions, and encouraging results were obtained. In this study, Al^{3+}, Ni^{+2}, and Cu^{+} metal ions were chosen and made to interact with BSA under physiological conditions (pH 7.4). Utilizing the FT-IR second derivative resolution enhancement approach, the associated binding interactions were investigated [13]. The findings of this study might offer new perspectives and insights on how copper (I), nickel (II), and aluminium (III) ion-based complexes would interact with the albumin protein along with their possible toxic effects.

2. Materials and Methods

2.1. Instruments and Chemicals. Metal salts aluminium (III) chloride ($AlCl_3$), nickel (II) chloride ($NiCl_2$), and copper (I) chloride (CuCl) were obtained from Sigma-Aldrich (Steinheim, Germany) and utilised as such. The BSA protein (>99.0%), acetic acid, and tris buffer were also purchased from Sigma-Aldrich (Steinheim, Germany) and were used without further purification. Throughout the study, ultrapure water (18 Ω), prepared in our lab using milli Q system (Millipore, Molsheim, France) was used. The FT-IR spectrum was obtained using a Nicolet iS10 FT-IR spectrophotometer (Thermo Fischer Scientific, Germany) equipped with a liquid nitrogen-cooled MCT detector. The absorption spectra for BSA-metal ion complexes were obtained using a double beam UV-visible spectrophotometer (Shimadzu, Japan).

2.2. Preparation of Solutions. To prepare the tris buffer (20 mM, pH 7.4), 1.21 g of precisely weighed tris powder was dissolved in 100 mL of pure deionized water, followed by an adjustment of the pH to 7.4 using a dilute acetic acid solution. The final volume of the resulting solution was adjusted to 500 mL using ultrapure deionized water. To prepare the BSA protein solution (0.5 mM), accurately weighed (1.65 g) BSA powder was dissolved in 50 mL of the freshly prepared tris buffer solution. Similarly, metal stock solutions (1 mM each) were prepared using the same tris buffer by dissolving appropriate quantities of metal salts in 50 mL of buffer. Further dilutions were made using the stock solutions in order to achieve concentrations of 0.25, 0.1, and 0.025 mM for each metal solution. All the solutions, including tris, BSA, and metal ions, were prepared fresh on each day of analysis.

2.3. Protein-Metal Ion Complexes Preparation. The protein-metal ion complexes were prepared by gradually adding the respective metal ion solution to the BSA solution at room temperature with continuous stirring. In order to study the

effect of metal ion concentration on the complexation process, three metal ion concentrations (0.125, 0.25, and 0.5 mM) were tested to achieve distinct complexes while the final protein concentration was maintained at 0.25 mM. To ensure adequate complexation between the test protein and metal ions, the combined solutions were incubated at 37°C for at least 2 h.

2.4. Fourier Transform-Infrared Spectroscopy (FTIR). The IR spectra of proteins alone and metal-protein complexes were obtained using hydrated films. Each sample was scanned 100 times at a resolution of 4 cm^{-1} in the transmittance range of 4000–400 cm^{-1}. The difference spectrum was used for subsequent analysis and was obtained by subtracting the spectrum of protein alone with the spectrum of protein-metal ion complexes [14].

2.4.1. Protein Conformational Analysis. Before and after interaction with various metal ions, the secondary structures of tested BSA protein were examined using FT-IR in a transmittance range of 1700–1600 cm^{-1} (amide band) [15]. The variation in intensities along with spectral shifting in the amide-A band, which corresponds to -NHstr. At 3500 cm^{-1}, amide I band for −C=O stretching at 1700–1650 cm^{-1}, and amide II band for C-N stretching coupled with -NH bending at 1550 cm^{-1}, before and after interaction with metal ions, were examined. The secondary structure of BSA proteins at amide I band including β-antiparallel (1691–1680 cm^{-1}), α-helix (1660–1650 cm^{-1}), β-turn (1678–1670 cm^{-1}), β-sheet (1637–1614 cm^{-1}), and random coil (1648–1638 cm^{-1}) were measured using the resolution enhancement method.

Gaussian functions were used to adjust the acquired values, and the corresponding peak areas were calculated for each secondary structure component. Origin Pro 2019 (Origin Lab, MA, USA) was used for self-deconvolution, and curve-fitting method was employed to investigate the metal-protein complexes and secondary structure of the protein. To determine the changes in protein after complexation, secondary structures of the protein were examined by computing the percentages of α-helix, random coil, β-sheet, β-turn, and β-antiparallel components. The % area of amide I components was calculated by multiplying the area corresponding to each band that characterises an amide I component by the overall area [16, 17]. Since the α-helix constitutes the largest component of amide I band, it was considered the basis for measuring metal-protein interaction, and the modification in the helical structure of BSA protein, was calculated using the equation below:

$$\%\ \text{change in}\ \alpha\ \text{helix} = \frac{\%\ \alpha\ \text{helix in BSA} - \text{metal ion complex} - \%\ \alpha\ \text{helix in BSA alone}}{\%\ \alpha\ \text{helix in BSA alone}} \times 100. \quad (1)$$

2.5. Ultraviolet-Visible Spectroscopy. The UV-Vis spectroscopic study to investigate the BSA-metal complexation was performed using previously reported methods [18, 19] with slight modifications. The 0.5 mM solution of BSA and 1 mM solutions of Copper (I), Nickel (II), and Aluminium (III) metal ions were prepared by mixing accurately weighed amounts of BSA and metal salts, respectively, in 20 mM of freshly prepared tris buffer (pH 7.4). BSA (24 μM) and the metal ion solutions were mixed appropriately in the same tris buffer to achieve effective concentrations of 8, 16, 24, 32, 40, 48, 56, and 64 μM. The BSA and metal ion solutions were mixed in equal volumes (1 : 1) at rt in such a way to achieve 0, 4, 8, 12, 16, 20, 24, 28, and 32 μM metal ion concentrations while the concentration of BSA was kept constant at 12 μM. The prepared solutions were mixed properly by shaking followed by incubation at room temperature (25 ± 2°C) for 2 h and subsequently at 37°C for 2 h. The absorption spectra of BSA-metal ions, complexes as well as BSA alone were recorded after incubation. To avoid the interference caused by absorption due to unreacted metal ions at the measured wavelength, the spectra of the complexes were subtracted from the spectra of metal ions.

2.5.1. Determination of Binding Constants. The binding constants (K) of BSA-metal complexes were calculated using a previously reported method [18, 19] using the absorbance data for BSA before and after formation of complexes with metal ions. If we assume only one type of interaction between the metal ions and BSA, the following equations (2) and (3) can be derived:

$$\text{BSA} + \text{metal} \Leftrightarrow \text{BSA: metal}, \quad (2)$$

$$K = \frac{\text{BSA: metal}}{[\text{BSA}]\,[\text{metal}]}, \quad (3)$$

where K = binding equilibrium constant of metal ion: BSA complexes.

If we consider BSA: metal as C_B

$$K = \frac{C_B}{(C_{\text{BSA}} - C_B)(C_{\text{metal}} - C_B)}, \quad (4)$$

where C_{metal} and C_{BSA} represent the concentrations of metal ions and BSA, respectively, in aqueous solution.

According to Beer–Lambert Law,

$$C_{\text{BSA}} = \frac{A_0}{\varepsilon_{\text{BSA}}.\ell}, \quad (5)$$

$$C_B = \frac{(A_0 - A)}{\varepsilon_B.\ell}, \quad (6)$$

where A_0 along with A represent the absorption values of BSA in the absence and presence of metal ions at 280 nm, respectively. ε_{BSA} and ε_B denote the molar extinction

coefficients of BSA and the bound metal ions, respectively, whereas the path length is assumed to be 1 cm.

The CBSA and CB values from equations (5) and (6) can now be replaced to (4) to derive the following equation:

$$\frac{A_0}{A_0 - A} = \frac{\varepsilon_{\mathrm{BSA}}}{\varepsilon_B} + \frac{\varepsilon_{\mathrm{BSA}}}{\varepsilon_B . K} \cdot \frac{1}{C_{\mathrm{Metal}}}. \quad (7)$$

A dual reciprocal plot across $1/C_{\mathrm{Metal}}$ on X-axis, along with $1/A_0 - A$ on Y-axis was plotted and the binding constants (K) were calculated using the intercept-to-slope ratio.

3. Results and Discussion

3.1. FT-IR Spectroscopic Analysis. The most prevalent blood protein, serum albumin, is engaged in a variety of physiological activities, including binding with drugs, especially metallodrugs. Plasma proteins are known to bind with metal ions, and the strength of the interaction depends on a number of factors, most importantly the type of metal ions. Some metal ions attach themselves to these plasma proteins strongly, while others bind weakly. By utilising this interaction, different metal-based drugs with a range of potential physiological effects can be designed. In this study, the interactions between group-A metal ions (Al^{+3}) along with heavy metal ions including Cu^{+} and Ni^{+2} with BSA were analyzed using FT-IR spectroscopy. Since metal ions and proteins interact to modify the structural and conformational properties of the protein, these changes can be examined using various spectroscopic methods. The FT-IR technique was applied to evaluate the properties of amide bands, and the variations in intensity and spectral shifting as a result of this interaction were measured. Before and after metal ion interaction, the amide I band of BSA protein was examined between the wave numbers 1700 and 1600 cm^{-1} (C=O stretching), the amide II band was examined at 1550 cm^{-1} (C-N stretching coupled with N-H band modes), and the amide A band was examined at 3500 cm^{-1} (NH stretching) [14, 17].

The secondary structure of the BSA protein was deconvoluted and analyzed using OriginPro 2019 graphing software, and various secondary structure components, including the β-antiparallel (1691–1680 cm^{-1}), β-turn (1678–1670 cm^{-1}), α-helix (1660–1650 cm^{-1}), random coil (1648–1638 cm^{-1}), and β-sheet (1637–1614 cm^{-1}) were investigated for spectral shift and intensity variations. The FT-IR spectrum of the free protein was subtracted from that of the BSA-metal complex to get the difference spectra. The FT-IR spectra were generated for both free BSA and for the BSA-metal complexes. Different spectra obtained were subsequently examined to determine how the peak intensities and wave numbers changed as the complex formed. The secondary structures of proteins were analyzed using self-deconvolution and curve-fitting techniques [15].

3.1.1. Interactions of BSA with Heavy Metal Ions (Cu^{+} and Ni^{+2}). Two heavy metal ions (Cu^{+} and Ni^{+2}) were selected for the investigation, and their interactions with BSA protein were measured at two different concentrations (0.125 mM and 0.5 mM). The lower metal ion concentrations did not produce significant results, as there were no marked differences in the spectra, indicating very weak interactions. On the contrary, higher metal ion concentrations resulted in good interactions as evident from the difference spectra shown in Figures 2(b) and 2(d). It was observed that the peak intensities in the difference spectra were good, indicating robust interactions between the metal ions and the BSA protein. The negative peaks in the difference spectra signified that the peak intensity decreased upon BSA-metal ion interaction, while the peaks in the positive region indicated an increase in the intensity.

The spectrum shift of NH_{str} peak, which in the case of free BSA was at 3308 cm^{-1}, was examined for the two complexes. Difference spectra of BSA-Cu^{+} and BSA-Ni^{+2} complexes are given in Figures 2(c) and 2(e). It was observed to be dramatically shifted to 3431 cm^{-1} in case of BSA-Cu^{+} complex and 3493 cm^{-1} for BSA-Ni^{+2} complex, indicating strong interaction of these metal ions with the BSA protein. These metal ions interacted with C-N and N-H functional groups of the protein, resulting in shifting of NH_{str} frequency. Additionally, the amide I band for free BSA was seen to shift to 1657 cm^{-1} and 1654 cm^{-1} for the BSA-Cu^{+} and BSA-Ni^{2+} complexes, respectively. This change was owing to a strong interaction between the metal ions and C-O group of the BSA protein. Moreover, the COO^{-} band in the case of free BSA at 1395 cm^{-1} was noticeably downshifted to 1374 cm^{-1} and 1390 cm^{-1} for BSA-Cu^{+} and BSA-Ni^{+2} complexes, respectively.

The secondary structures of free BSA and the BSA-metal ion complexes were quantitatively determined over the range 1700–1600 cm^{-1}, and the conformational changes induced by metal ions were evaluated. Figure 3 depicts the second derivative resolution enhancement and curve-fitted model for the amide I band over the spectral range 1700–1600 cm^{-1} and Table 1 summarizes the percentages of secondary structure components calculated for free BSA as well as the BSA-metal ion complexes. It is evident from Table 1 that upon complexation, the percentages of several components, including β-turn, β-antiparallel, random coil, β-sheet, and α-helix varied. The proportions of secondary structure components calculated for free BSA were found to be consistent with the previously reported results [20].

In comparison to BSA alone, which showed a α-helix content of 62%, the values calculated for the BSA-Cu^{+} and BSA-Ni^{+2} complexes were calculated to be 44% and 48%, respectively. This suggested a marked reduction in α-helix component of BSA protein upon interaction with the metal ions. Additionally, the random coil component increased from 5% for free BSA to 21% and 13% for BSA-Cu^{+} and BSA-Ni^{+2} complexes, respectively. Also, the β-antiparallel component considerably increased from 3% (free BSA) to 8% (BSA-Cu^{+}) and 7% (BSA-Ni^{2+}), indicating a strong interaction between the two heavy metal ions and BSA protein (Figures 3(a)–3(c)).

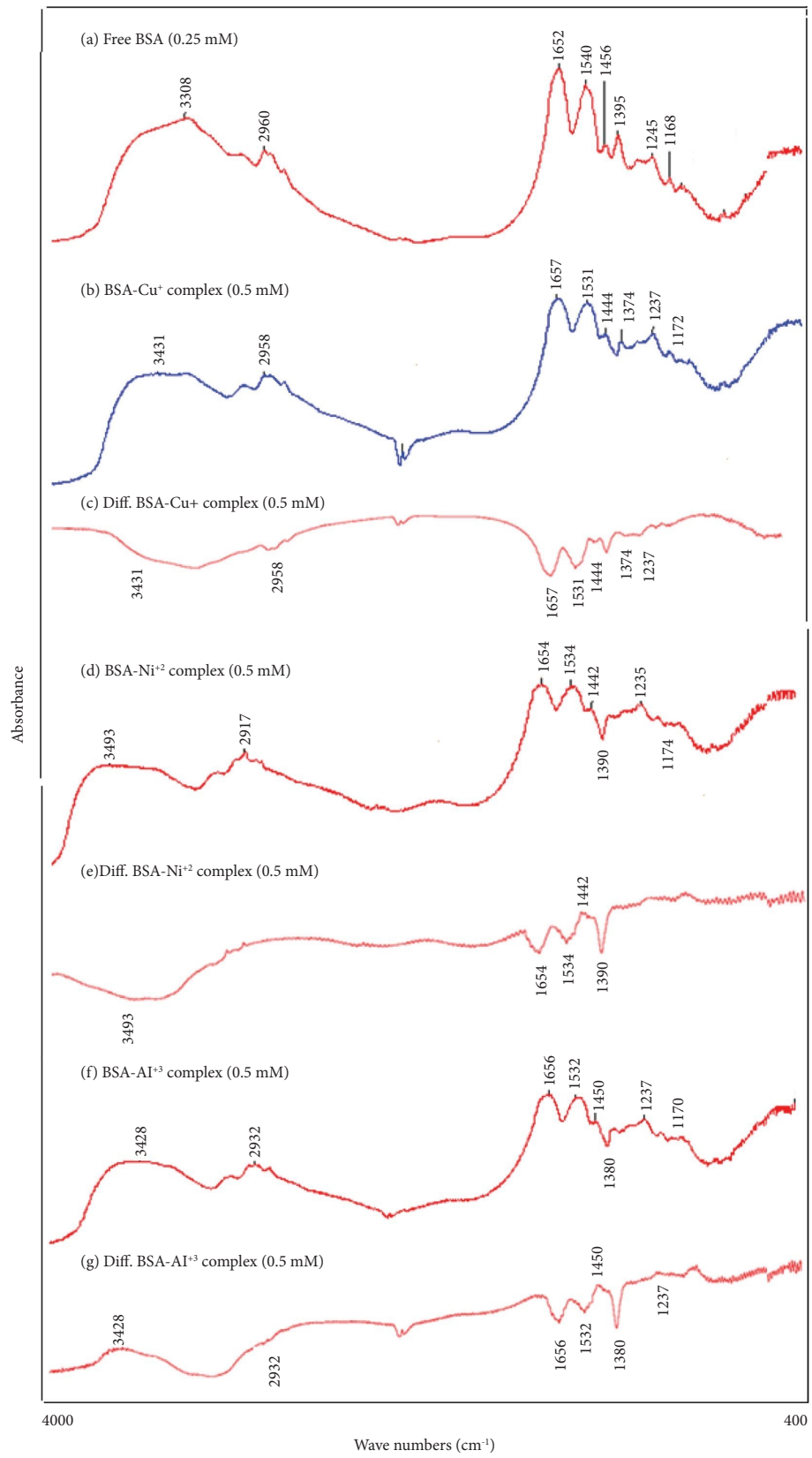

Figure 2: Fourier transform IR spectra of (a) unbound BSA, (b) BSA-Cu complex (0.5 mM), (c) differential complex of BSA-Cu (0.5 mM), (d) complex of BSA-Ni (0.5 mM), (e) differential complex of BSA-Ni (0.5 mM), (f) complex of BSA-Al (0.5 mM), and (g) differential complex of BSA-Al (0.5 mM).

Table 1: Secondary structural study of the Cu^{+}, Ni^{+2}, and Al^{+3} complexes of free BSA.

Amide I (cm^{-1}) components	Free BSA (%) 0.25 mM	BSA-Al^{+3} complex (%) 0.5 mM	BSA-Cu^{+} complex (%) 0.5 mM	BSA-Ni^{+2} complex (%) 0.5 mM
β–sheet (±2) 1614–1637	14	15	15	18
Random coil (±2) 1638–1648	5	20	21	13
α–helix (±4) 1650–1660	62	46	44	48
β–turn (±2) 1670–1678	16	12	12	14
β–antiparallel (±1) 1680–1691	3	7	8	7

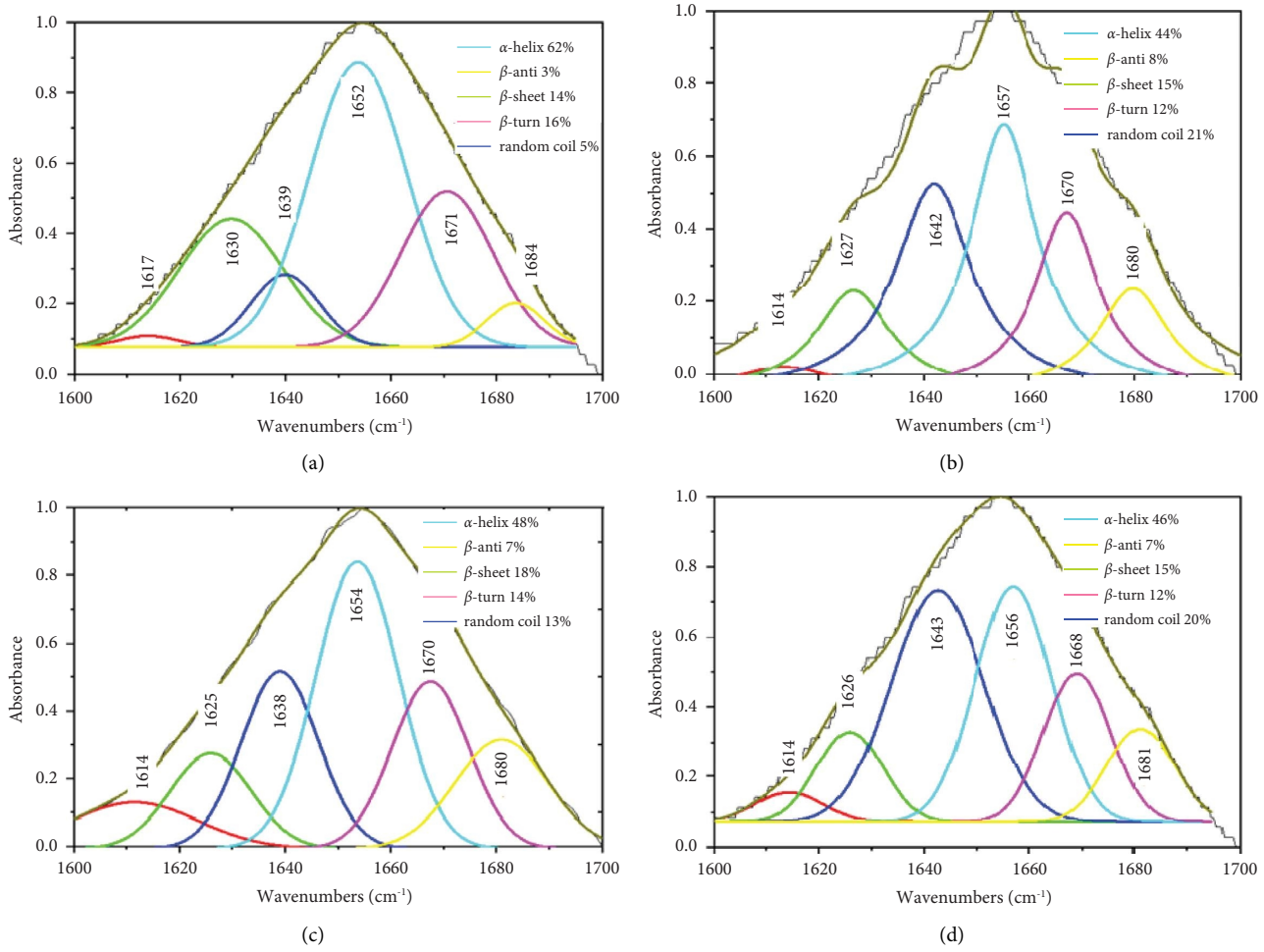

Figure 3: For (a) free BSA, curve fitted amide I at 1700–1600 cm^{-1} ($R^2 = 0.99$). (b) BSA-Cu^{+}. (c) BSA-Ni^{+2}. (d) complexes of BSA-Al^{+3}.

3.1.2. BSA Interaction with Group A Metal Ions (Al^{+3}). A known concentration of BSA (0.25 mM) was made to interact with two different Al^{+3} metal ion concentrations of 0.125 mM and 0.5 mM under physiological conditions. Spectra for free BSA and BSA-Al^{3+} complexes along with their difference spectrums are given in Figures 2(a), 2(f), and 2(g). Similar to the heavy metal ions, the lower Al^{3+} metal concentration did not show a marked change in the spectrum, indicating a nonsignificant interaction with the BSA protein. However, at higher metal ion concentrations (0.5 mM), considerable interaction was observed as evident from positive and negative peaks of good intensities in the difference spectra. The negative peaks of the amide I and amide II bands in the difference spectrum revealed that the spectral intensities markedly decreased following interaction. This decrease in the spectral intensity was due to the decrease in its α-helical component [21]. In the case of the BSA-Al^{3+} complex, two negative peaks with good intensities at 1656 cm^{-1} along with 1532 cm^{-1}, corresponding to the amide I and amide II, respectively were observed in the difference spectrum. Since Al^{3+} is a hard acid, it might have reacted with the C=O, COO^{-}, and NH groups of BSA, based on the Hard and Soft Acid Base (HSAB) theory of binding [8, 9, 22, 23].

The spectral shift of the NH_{str} peak from 3308 cm^{-1} in the case of free BSA to 3428 cm^{-1} for BSA-Al^{3+} complex further supported these binding interactions. This considerable NH_{str} shift suggested that the Al^{3+} ions interacted with the C-N and N-H groups of the protein. Additionally,

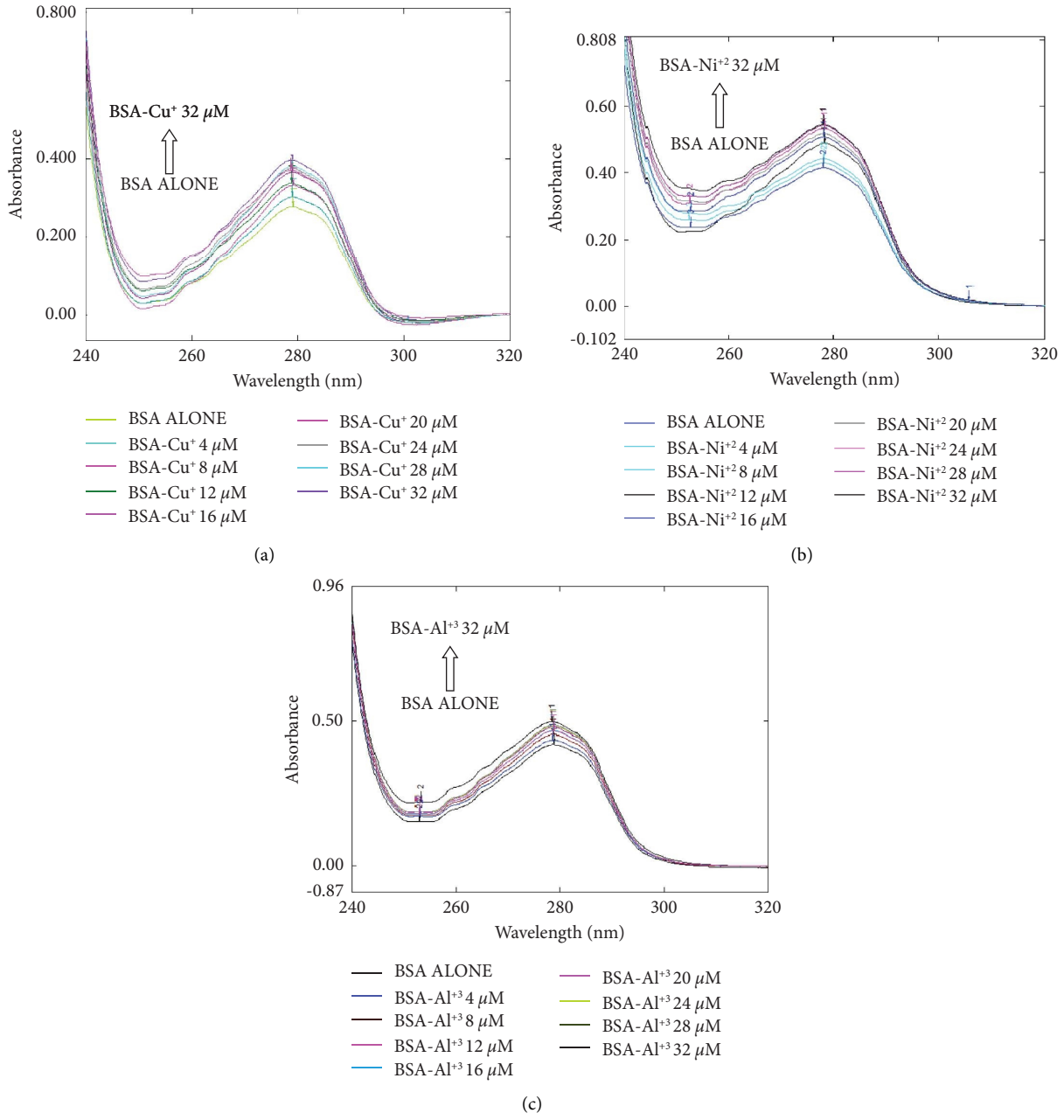

FIGURE 4: Spectral overlay showing increasing concentrations of (a) Cu^{+}, (b) Ni^{+2}, and (c) Al^{+3} ions on BSA's ability to absorb UV light; tris buffer; $C_{BSA} = 12\,\mu M$; $C_{metal} = 0$, 4, 8, 12, 16, 20, 24, 28, and $32\,\mu M$ (pH 7.4).

the BSA-metal complex showed a change in the amide I band from $1652\,cm^{-1}$ in free BSA to $1656\,cm^{-1}$, demonstrating good interaction between the C-O group of BSA protein and Al^{3+} metal ions. A downshift was also observed in the COO^{-} band which changed from $1395\,cm^{-1}$ for free BSA to $1380\,cm^{-1}$ for the BSA-Al^{3+} complex. The secondary structure analysis of BSA-Al^{3+} complex showed a marked decrease in the α-helical content from 62% to 46% as well as in the β-turn (from 16% to 12%). However, the percentages of random coil and β–antiparallel increased significantly from 5% to 3% in free BSA to 20% and 7% for BSA-Al^{+3} complex, respectively (Figure 3(d), Table 1).

3.2. Ultraviolet Spectroscopic Analysis. UV-Vis spectroscopy is a rapid and efficient method for the measurement of protein-ligand binding and protein conformational changes [24]. It was based on the measurement of absorption spectra of BSA alone and its complexes with Cu^{+}, Ni^{+2}, and Al^{3+} ions. The results showed a sharp absorption peak of BSA at 280 nm, which increased in the intensity as the metal ion concentrations increased from 4 to $32\,\mu M$ (figures 4(a)–4(c)). The tryptophan residue present on the surface of the BSA protein might have interacted with the metal ions via electrostatic interactions which resulted in a hyperchromic shift [25].

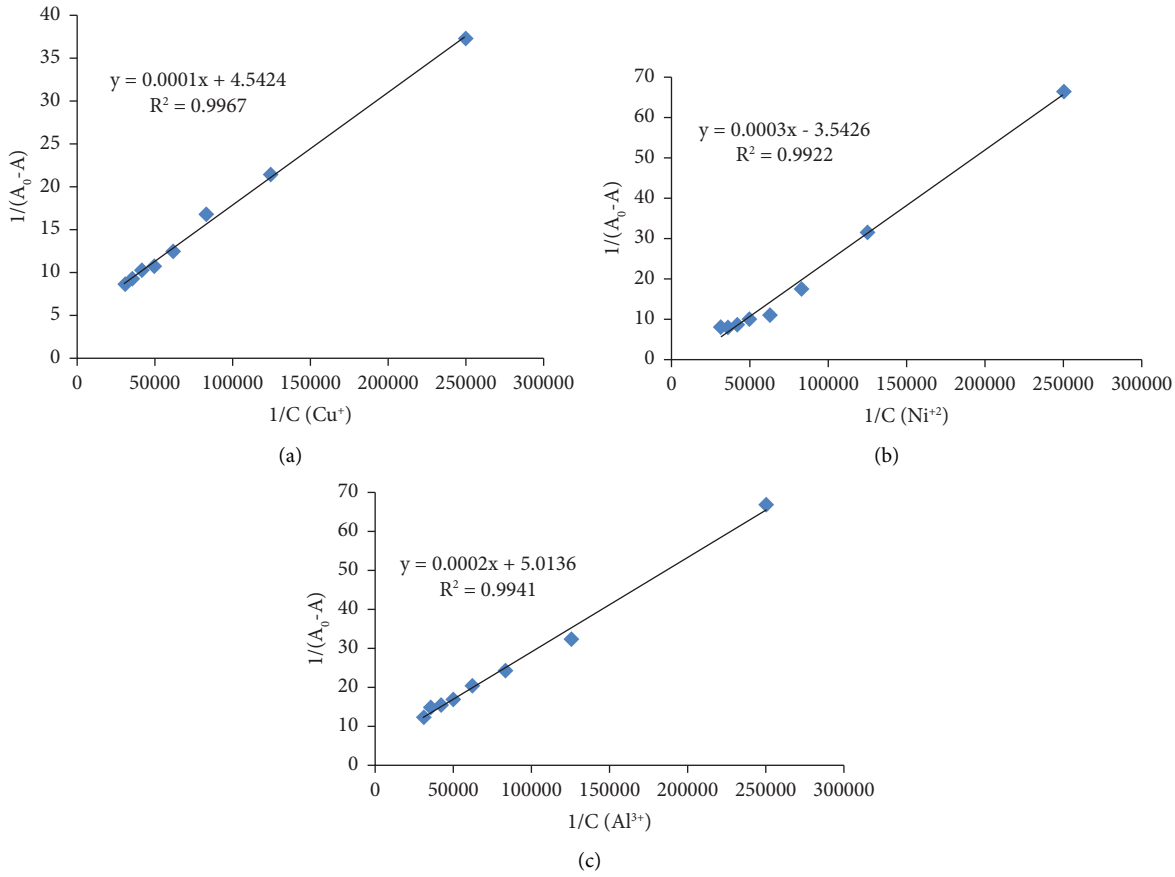

Figure 5: Plot of $1/(A_0 - A)$ vs. $1/C_{metal}$; A_0 and A = the absorbance of BSA alone and BSA-metal complexes, respectively; C_{metal} = concentration of Cu^+, Ni^{+2}, and Al^{+3}. Buffer: tris (pH 7.4); $C_{BSA} = 12\,\mu M$; $C_{metal} = 0$, 4, 8, 12, 16, 20, 24, 28, and $32\,\mu M$; (a) $K_{Cu+} = 3.46 \times 10^4\,M^{-1}$, (b) $K_{Ni}{}^{2+} = 1.28 \times 10^4\,M^{-1}$, and (c) $K_{Al}{}^{3+} = 2.08 \times 10^4\,M^{-1}$ are the binding constants.

Table 2: Comparison of metal ions-protein interaction results from FT-IR and UV-Vis spectroscopy with those from ACE.

Metal ions	$\Delta R/R_f \pm cnf$ values in ACE* [1]	% variation in α-helix after complexation	Binding constant (M^{-1})
Cu^+	-0.0754 ± 0.0088	−29.03	3.46×10^4
Al^{+3}	-0.0484 ± 0.0087	−25.80	2.08×10^4
Ni^{+2}	-0.0397 ± 0.0037	−22.58	1.28×10^4

*ΔR: the mobility ratios of BSA in a capillary with and without metal ions vary. R_f: the mobility fraction of BSA in the lack of metal ions. *Cnf*: confidence interval calculated for six replicate tests.

To measure the extent of interaction of metal ions with the BSA protein, binding constants were calculated for the BSA-Cu+, BSA-Ni^{+2}, and BSA-Al^{+3} complexes and were found to be $3.46 \times 10^4\,M^{-1}$, $1.28 \times 10^4\,M^{-1}$, and $2.08 \times 10^4\,M^{-1}$, respectively (Figures 5(a)–5(c)). As reported earlier, the ideal binding constant should be between 10^4 and $10^6\,M^{-1}$ [1], and the ligands with their binding constant values in this range are believed to be suitable for drug development. As the metal ions also showed binding constants in this range, they and their metal-based ligands are expected to effectively bind to the BSA protein and distribute themselves throughout the biological system.

3.3. Comparison of FT-IR and UV Findings with ACE. The findings of this investigation were compared with those of an earlier study of similar nature, which was conducted by our group utilising affinity capillary electrophoresis (ACE) [8]. The interactions of five distinct proteins, including BSA, with numerous physiologically significant metal ions were measured using ACE. Protein mobility shift following the interaction was measured in order to evaluate the interaction. The percentage change in theα-helical structure of BSA after interaction with metal ions and the binding constants of the complexes were used to compare with the mobility shift data obtained using ACE (Table 2). As evident from Table 2, the outcomes of all three methods were similar

and showed comparable findings. It could be observed that the Cu^{+} ion exhibited the strongest interaction with BSA, and this fact was supported by both techniques. In all three employed methods, the degree of interaction decreased in the order $Cu^{+} < Al^{3+} < Ni^{2+}$.

4. Conclusions

The current study was aimed to develop a simple, rapid, cost-effective, and accurate method to measure the interaction between metal ions and BSA protein. Simple spectroscopic techniques such as FT-IR and UV-Vis were successfully employed in this study to assess the interactions of several distinct biologically significant metal ions with BSA. These techniques has many advantages over sophisticated techniques, as they do not require tedious sample preparation steps and not much expertise is needed making them cost-effective techniques which can be used for routine analysis of metal-protein or drug-protein interactions. These techniques were also found to be accurate as the results were comparable with the ACE technique used earlier to measure the interaction. However, these techniques have some limitations, as they might not be as sensitive as the high-end instruments, and therefore, they can only be utilised for routine analysis. Also, these techniques give preliminary data about the interaction with BSA, and further mechanistic investigations are required to establish the mechanism of binding of these metal ions with the binding site present in the BSA protein.

Data Availability

The data that support the findings of this study are available from the corresponding author, [MSA], upon reasonable request.

Conflicts of Interest

The authors declare that they have no conflicts of interest.

Acknowledgments

The authors extend their appreciation to the Deputyship for Research & Innovation, Ministry of Education in Saudi Arabia for funding this Research work through the project number: ISP22-12.

References

[1] H. A. Alhazmi, M. Al Bratty, A. M. Meraya et al., "Spectroscopic characterization of the interactions of bovine serum albumin with medicinally important metal ions: platinum (IV), iridium (III) and iron (II)," *Acta Biochimica Polonica*, vol. 68, no. 1, pp. 99–107, 2021.

[2] H. A. Alhazmi, "FT-IR Spectroscopy for the identification of binding sites and measurements of the binding interactions of important metal ions with bovine serum albumin," *Scientia Pharmaceutica*, vol. 87, no. 1, p. 5, 2019.

[3] Y. W. Lin, "Rational design of artificial metalloproteins and metalloenzymes with metal clusters," *Molecules*, vol. 24, no. 15, p. 2743, 2019.

[4] S. E. Harding and B. Z. Chowdhry, *Protein-Ligand Interactions: A Practical Approach Volume 1: Hydrodynamics and Calorimetry*, Oxford University Press Inc, New York, NY, USA, 2001.

[5] H. Alyar, S. Alyar, A. Unal, N. Ozbek, E. Şahin, and N. Karacan, "Synthesis, characterization and antimicrobial activity of m-toluenesulfonamide, N,N′-1,2-ethanediylbis (mtsen) and [Cu(II)(phenanthroline)2]mtsen complex," *Journal of Molecular Structure*, vol. 1028, pp. 116–125, 2012.

[6] D. Witkowska and M. Rowińska-Żyrek, "Biophysical approaches for the study of metal-protein interactions," *Journal of Inorganic Biochemistry*, vol. 199, Article ID 110783, 2019.

[7] Y. Cao, K. S. Er, R. Parhar, and H. Li, "A force-spectroscopy-based single-molecule metal-binding assay," *ChemPhysChem*, vol. 10, no. 9-10, pp. 1450–1454, 2009.

[8] H. A. Alhazmi, M. Nachbar, H. M. Albishri et al., "A comprehensive platform to investigate protein-metal ion interactions by affinity capillary electrophoresis," *Journal of Pharmaceutical and Biomedical Analysis*, vol. 107, pp. 311–317, 2015.

[9] H. A. Alhazmi, M. Al Bratty, S. A. Javed, and K. G. Lalitha, "Investigation of transferrin interaction with medicinally important noble metal ions using affinity capillary electrophoresis," *Pharmazie*, vol. 72, no. 5, Article ID 29441867, pp.; 248, 2017.

[10] H. A. Alhazmi, "Measurement of interaction behavior of six biologically important noble metal ions with the iron(III) binding protein, apo-transferrin, using mobility-shift affinity electrophoresis," *Pharmazie*, vol. 73, no. 3, pp. 143–149, 2018.

[11] H. A. Alhazmi, S. A. Javed, W. Ahsan et al., "Investigation of binding behavior of important metal ions to thioredoxin reductase using mobility-shift affinity capillary electrophoresis: a preliminary insight into the development of new metal-based anticancer drugs," *Microchemical Journal*, vol. 145, pp. 259–265, 2019.

[12] M. Al Bratty, H. A. Alhazmi, A. Najmi et al., "Spectroscopic studies for Rhodium (III) binding to apo-transferrin," *Journal of Chemistry*, vol. 2022, Article ID 2879840, 10 pages, 2022.

[13] U. S. Akshath, P. Bhatt, and S. A. Singh, "Differential interaction of metal ions with gold nanoclusters and application in detection of cobalt and cadmium," *Journal of Fluorescence*, vol. 30, no. 3, pp. 537–545, 2020.

[14] S. H. Rutherford, G. M. Greetham, A. W. Parker, A. Nordon, M. J. Baker, and N. T. Hunt, "Measuring proteins in H_2O using 2D-IR spectroscopy: pre-processing steps and applications toward a protein library," *Journal of Chemical Physics*, vol. 157, no. 20, Article ID 205102, 2022.

[15] D. M. Byler and H. Susi, "Examination of the secondary structure of proteins by deconvolved FTIR spectra," *Biopolymers*, vol. 25, no. 3, pp. 469–487, 1986.

[16] R. Nagao, T. Tomo, and T. Noguchi, "Effects of extrinsic proteins on the protein conformation of the oxygen-evolving center in cyanobacterial photosystem II as revealed by Fourier transform infrared spectroscopy," *Biochemistry*, vol. 54, no. 11, pp. 2022–2031, 2015.

[17] D. Despotović, L. M. Longo, E. Aharon et al., "Polyamines mediate folding of primordial hyperacidic helical proteins," *Biochemistry*, vol. 59, no. 46, pp. 4456–4462, 2020.

[18] D. S. Reddy, M. Kongot, V. Singh et al., "Coumarin tethered cyclic imides as efficacious glucose uptake agents and investigation of hit candidate to probe its binding mechanism with human serum albumin," *Bioorganic Chemistry*, vol. 92, Article ID 103212, 2019.

[19] C. Puscas, A. Mircea, M. Raiu, M. Mic, A. A. A. Attia, and R. Silaghi-Dumitrescu, "Affinity and effect of anticancer drugs on the redox reactivity of hemoglobin," *Chemical Research in Toxicology*, vol. 32, no. 7, pp. 1402–1411, 2019.

[20] I. Yousuf, M. Bashir, F. Arjmand, and S. Tabassum, "Multi-spectroscopic insight, morphological analysis and molecular docking studies of Cu^{II}-based chemotherapeutic drug entity with human serum albumin (HSA) and bovine serum albumin (BSA)," *Journal of Biomolecular Structure and Dynamics*, vol. 37, no. 12, pp. 3290–3304, 2019.

[21] Y. Wu, L. Chen, J. Chen et al., "Covalent binding mechanism of Furmonertinib and Osimertinib with human serum albumin," *Drug Metabolism & Disposition*, vol. 51, no. 1, pp. 8–16, 2023.

[22] A. Evans and K. A. Kavanagh, "Evaluation of metal-based antimicrobial compounds for the treatment of bacterial pathogens," *Journal of Medical Microbiology*, vol. 70, no. 5, Article ID 001363, 2021.

[23] R. A. Miranda-Quintana and J. Smiatek, "Application of fundamental chemical principles for solvation effects: a unified perspective for interaction patterns in solution," *Journal of Physical Chemistry B*, vol. 126, no. 43, pp. 8864–8872, 2022.

[24] A. Singh, A. Kumar, P. Kumar, T. Bhardwaj, R. Giri, and N. Garg, "Salvianolic acid B noncovalently interacts with disordered c-Myc: a computational and spectroscopic-based study," *Future Medicinal Chemistry*, vol. 13, no. 16, pp. 1341–1352, 2021.

[25] M. Zhou, Y. Bi, H. Zhou et al., "Aggregation behavior of poly (acrylic acid-co-Octadecyl methacrylate) and bovine serum albumin in aqueous solutions," *ChemistryOpen*, vol. 10, no. 3, pp. 373–379, 2021.